Fluid–fluid–solid triple point on melting curves at high temperatures

G E Norman and I M Saitov

Joint Institute for High Temperatures of the Russian Academy of Sciences, Izhorskaya 13 Bldg 2, Moscow 125412, Russia

E-mail: genri.norman@gmail.com

Abstract. An analysis is presented of experimental data where fluid–fluid phase transitions are observed for different substances at high temperatures with triple points on melting curves. Viscosity drops point to the structural character of the transition, whereas conductivity jumps remind of both semiconductor-to-metal and plasma nature. The slope of the phase equilibrium dependencies of pressure on temperature and the consequent change of the specific volume, which follows from the Clapeyron–Clausius equation, are discussed. $P(V,T)$ surfaces are presented and discussed for the phase transitions considered in the vicinity of the triple points. The cases of abnormal $P(T)$ dependencies on curves of phase equilibrium are in the focus of discussion. In particular, a $P(V,T)$ surface is presented when both fluid–fluid and melting $P(T)$ curves are abnormal. Particular attention is paid to warm dense hydrogen and deuterium, where remarkable contradictions exist between data of different authors. The possible connection of the $P(V,T)$ surface peculiarities with the experimental data uncertainties is outlined.

1. Introduction

Two predictions are formulated by Norman and Starostin [1,2] in 1968. The first one is "plasma phase transition". Current situation on the problem is discussed in [3]. The second prediction is a fluid–fluid–solid triple point on a melting curve at high temperatures. Such a triple point is observed experimentally first by Brazhkin et al [4] for selenium in 1989. The nature of the fluid–fluid transition at the triple point is not discussed in [1, 2]. The authors [4] look for a semiconductor-to-metal transition.

Problems of the fluid–fluid–solid triple point are discussed in this work. An analysis is given briefly in section 2, specific cases observed are classified. Different opinions on the nature of the phase transition are presented in section 3. Section 4 is devoted to the particular 3D shapes of the thermodynamic $P(V,T)$ surfaces,where P is pressure, V is specific volume, T is temperature. The important case of warm dense hydrogen and deuterium, where remarkable contradictions exist between data of different authors, is considered in section 5. The possible connection of the $P(V,T)$ surface peculiarities with the experimental data uncertainties is outlined.

2. Analysis of experimental observations

2.1. Common case

A liquid–liquid–solid triple point is observed experimentally first in 1989 by Brazhkin with coauthors [4] for selenium at pressure in the region to the less values from the extremum point of the melting curve. The coexistence curve for the liquid–liquid phase transition is

diagnosed by the remarkable isobaric jumps of conductivity and viscosity and by a slight jump of the specific volume [4–7]. Brazhkin with coauthors extended their approach to some other elements. Coexistence curve for the liquid–liquid phase transition and corresponding liquid–liquid–solid triple points are observed for tellurium, tin, sulphur and bismuth, see [5] for the references. Tellurium is the only element for which the short-range order structure changes during metallization of the melt are reliably established by means of neutron scattering. This transformation is accompanied by a decrease of volume and resistivity.

They use the term "liquid" since triple point temperatures are below the critical ones. A solid-solid-liquid triple point is supposed to exist adjacent to liquid–liquid–solid triple point on the melting curve.

2.2. Sulphur and bismuth

The phase diagram of sulphur is considered in [5] to be the most complicated of all elements. More than ten solid phases of S and numerous anomalies are found. Two liquid–liquid–solid triple points are observed. The first liquid–liquid coexistence curve is established as a result of thermobaric analysis and resistivity measurements. A reversible resistivity decrease by 2–3 orders of magnitude is accompanied by a volume decrease. The second transition takes place in the insulator region of the melt; a decrease of volume is obtained during the liquid–liquid transformation using the thermobaric analysis method.

Bismuth is an example of another exceptional case. Three liquids are observed as in sulphur. However, contrary to sulphur, there is a liquid–liquid-liquid triple point. It is located on the liquid–liquid coexistence curve which ends by the conventional liquid–liquid–solid triple point. In other words, there is a bifurcation of the initial liquid–liquid coexistence curve.

2.3. Metastability as a crucial proof

A phenomenon of metastability is an inherent indication of the first-order phase transitions. To check the existence of metastable states is important in particular when the volume decrease is relatively small as in the case of the liquid–liquid phase transitions analyzed. To resolve the problem, the kinetics of the transitions in melts of Se and S is investigated at different cooling rates dT/dt [8]. Superheating and supercooling of the liquid phases are seen at $dT/dt > 6\,\mathrm{K/s}$. Shifts of the transition curves are obtained. The curves are displaced by 15–30 K at $dT/dt > 40\,\mathrm{K/s}$, so the lifetime of the metastable states can be estimated as 0.1–1 s.

2.4. "Brazhkin-type" transitions

The discovery [4–7] initiates studies for different substances. An experimental observation of a liquid–liquid transition in phosphorus, involving an abrupt, pressure-induced structural change between two distinct liquid forms, is reported in [9,10]. The first experimental observation of a liquid–liquid phase transition in the monatomic liquid metal cerium is reported in [11]. Pressure-induced structural changes are found experimentally in poly (4-methyl-1-pentene) melt [12].

3. Nature of the transition

3.1. Diversity of interpretations

The pioneer experiment [4] is motivated by the search for the semiconductor-to-metal transition. The conductivity drops could also be related to a metallization or plasma phase transition.

However, structural changes are observed from the first experiments [5], and not only for tellurium mentioned above with its short-range order structure changes. Long molecular chains (up to 104 atoms per chain) [5] and Se_n rings (with n several times less than in chains) [13] are presented in liquid Se. Viscosity drop measured points to a drastic structural reconstruction of Se melt at the phase transition. The authors [9,10] report an in situ x-ray diffraction observation of

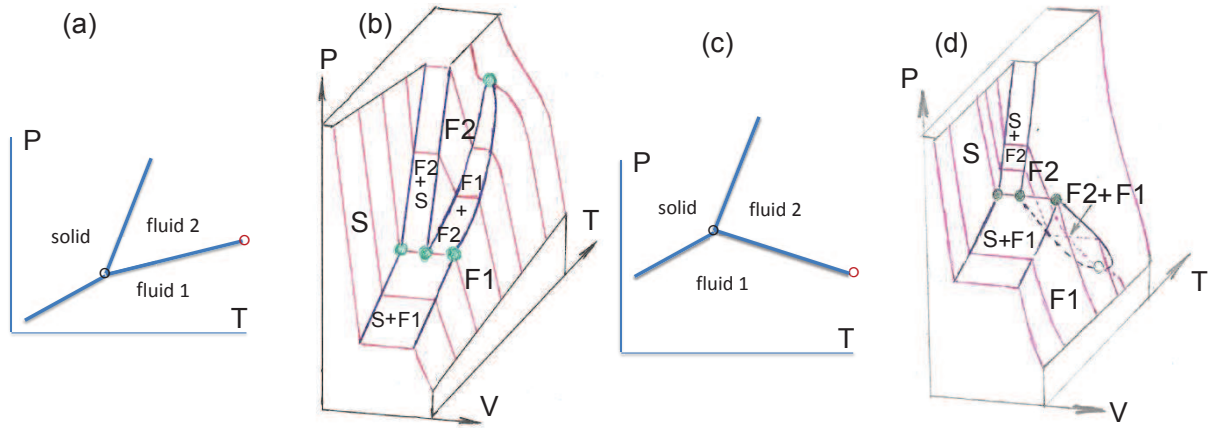

Figure 1. Schematic phase diagrams: (b)—thermodynamic $P(V,T)$ surface for the normal cerium case when the slopes of both melting and fluid–fluid coexistence curves $P(T)$ are positive (a). (d)—thermodynamic $P(V,T)$ surface for the abnormal Selenium case when the slope of the melting curve $P(T)$ is positive and the slope of the fluid–fluid coexistence curve $P(T)$ is negative (c). Isotherms are presented by red lines. S is solid, F is fluid.

a liquid–liquid transition in phosphorus, involving an abrupt, pressure-induced structural change between two distinct liquid forms.

3.2. Frenkel and Widom lines

Critical point for the liquid–liquid transition is not observed clearly in any substance but iron [14]. Therefore, some of the experimental findings concerning coexistence curve could be attributed to the lines of Frenkel or Widom type [15–21]. It is shown that the supercritical region of a liquid consists of not only one single state. Different states can differ one from another by the local structure or by some fitches of the molecule motion at small time scales [16] with crossover lines between them. Two lines on temperature-density plain separate regions of phase diagram where fluid shows different behavior related to collective particle motion [18]. The effect is a universal one since it is common for the supercritical both Lennard-Jonnes fluid, and iron melt [19], and carbon dioxide [20], and polar fluids [21].

It is necessary to emphasize that lines of Frenkel or Widom type do not have metastable states adjacent to them. Therefore, the existence of metastable states provides a strong experimental evidence for the first-order nature of transitions.

4. 3D thermodynamic $P(V,T)$ surfaces

4.1. Clapeyron–Clausius relation

On a P–T diagram, the line separating the two phases is known as the coexistence curve. The Clapeyron–Clausius relation gives the slope of the tangents to this curve,

$$\mathrm{d}T/\mathrm{d}P = T\Delta v/L, \tag{1}$$

where dT/dP is the slope of the tangent to the coexistence curve at any point, L is a specific latent heat of the phase transition, Δv is a specific volume change of the phase transition.

The slope of the phase equilibrium dependencies of pressure on temperature and the consequent change of the specific volume, which follows from the Clapeyron–Clausius equation, define 3D thermodynamic $P(V,T)$ surfaces. Schematic $P(V,T)$ surfaces are given in figures 1a–1d for the fluid–fluid phase transitions considered in the vicinity of the triple points. We use

the term fluid, as in abstract and introduction, in order not to be restricted to the case when the triple point temperature is less than the critical temperature of the liquid-vapor transition.

4.2. Iron

Measurements of electrical resistivity and caloric equation of state are performed for fluid iron to investigate the metal-to-nonmetal transition induced by thermal expansion [14]. The equation of state results reported provide strong evidence for the existence of a first-order phase transition with a critical point about 5 GPa and a density 4 times lower than the solid iron density at normal conditions. The critical point is found near the metal-to-nonmetal transition threshold. Contrary to other substances analyzed, volume decrease is evident and large. However, only near-critical region far from the triple point is investigated and temperature is not measured.

5. Warm dense hydrogen

5.1. Diversity of experimental approaches

Experimental results for warm dense hydrogen [22–30] and deuterium [22, 23, 27, 31, 32] are presented in figure 2. The melting curve results are given for the comparison.

A conducting fluid phase of hydrogen is achieved by the dynamic compression at density 0.64 mole/cm^3, pressure 140 GPa, temperature 2600 K in experiments with 100 ns lifetimes [22, 23] (star with error bar in figure 2). Conducting fluid deuterium is observed at shock compression; resistivity decreases 4–5 orders of magnitude just in the density range where the 20% increase of density is demonstrated [31]. There are several considerably different theoretical estimations of temperature for experimental values of density and pressure in [31]: temperatures obtained within the Saha-D model [33] are depicted by open hexagons; open triangles correspond to temperatures obtained in [34]; temperatures predicted within the framework of the model [35] are depicted by open squares.

The data [25] are obtained with a laser-driven shock wave in a hydrogen sample, pre-compressed in a diamond anvil cell. Optical reflectance probing reveals the onset of the conducting fluid state. Colored triangles in figure 2 correspond to measurements of the reflectance drops at wavelength 1064 nm [25]. Pulsed-laser heating above the melting curve of hydrogen at static pressures is used in the megabar pressure region [29, 30, 36]; the anomaly observed in the heating curve is interpreted as an indication to the phase transition. Both [29,30] and [31] focus on a first-order phase transition that should separate two distinct coexisting phases of hydrogen or deuterium which differ in density, conductivity, degree of ionization.

The authors [32] present the results of a series of dynamic compression experiments on liquid deuterium performed at the Sandia Z machine. These experiments show a dramatic increase in reflectivity of the deuterium samples, indicative of an abrupt increase in conductivity between 280 and 305 GPa, temperature remaining below 1800 K. The authors [32] interpret this signal as evidence of an abrupt, density-driven insulator-to-metal transition. Possibility of the specific volume drop is not studied in either [25] or [32].

Figure 2 shows dramatic contradictions which exist between data of different authors. The scatter of pressures achieves a factor 3. Possible metastability is not discussed. The pressures and temperatures of the fluid–fluid coexistence curve are much higher than the values of the critical point of hydrogen. It is fluid hydrogen.

5.2. Phase diagrams

The extremum of the experimental melting curve is about 1000 K and 100 GPa [24, 26–28]. The fluid–fluid–solid triple point is only a suggestion since it is obtained by extrapolation [22–32]. It is located at higher pressures than the extremum of the melting curve at the negative slope of melting curve, in contrast to the cases considered in section 2. The corresponding solid-solid-solid triple point is not clear, unlike in the cases in section 2. The nature of the transition

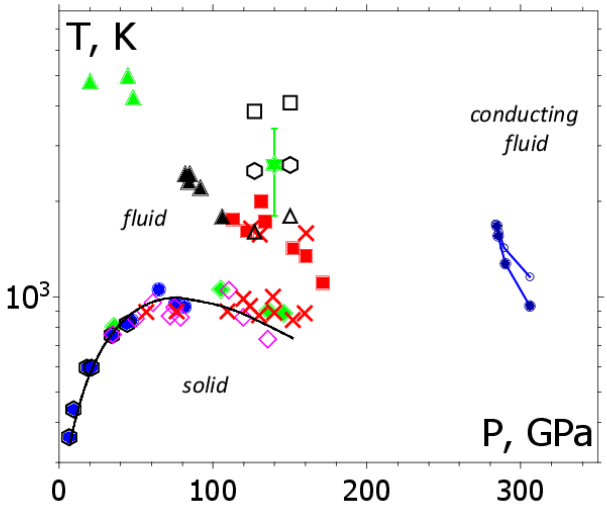

Figure 2. Experimental data for the solid–fluid and fluid–fluid phase coexistences in warm dense hydrogen and deuterium. Melting curve: blue hexagons [24], blue circles [26], open diamonds [28] for hydrogen; blue diamonds correspond to experimental data on melting of hydrogen and deuterium [27]; the line is drawn in order to guide the eye. Data on solid–fluid and fluid–fluid phase transition in hydrogen obtained in [29] are depicted by red crosses. Fluid–fluid phase transition: red squares [30]; black colored triangles [36]; green star with the error bar [22, 23] (hydrogen and deuterium); green triangles [25] (hydrogen). Fluid–fluid phase transition in deuterium observed in [31] with different theoretical methods for estimations of temperatures: open triangles [34]; open hexagons [33], open squares [35]. Circles connected by lines correspond to insulator-to-metal transition in fluid deuterium obtained in [32] with temperatures estimated: without taking into account of the latent heat (open circles); with latent heat (solid blue circles).

is under discussion [3]. The lower critical point of the fluid–fluid coexistence curve cannot be excluded.

Both positive and negative slopes of the fluid–fluid coexistence curve $P(T)$ can be consistent with the results of the measurements. The corresponding 3D pictures for the thermodynamic $P(V,T)$ surfaces are presented in figure 3. $P(V,T)$ surface is shown in figures 3c and 3d, when both fluid–fluid and melting $P(T)$ curves are abnormal. Theoretical estimations predict the negative slope [29, 30, 32, 37]. Structural transformations adjacent to the electronic transition complicate the theory [38].

It is important to emphasize that not only isotherms but both isobars, and isochors, and adiabatic and Hugoniot curves, and isentropes, and curves of all the possible processes are placed on the same $P(V,T)$ surfaces as isotherms. It means that if there is a break on the isotherm, the break takes place on the curves of all other processes. The situation needs special consideration only if the process is so extremely fast that the system loses the state of the local equilibrium.

5.3. Discussion

The possible connection of $P(V,T)$ surface peculiarities with the experimental data uncertainties is outlined. For instance, there is an uncertainty in interpretation of the experimental data on fluid–fluid phase transition in deuterium [22,23,31] associated with theoretical determination of

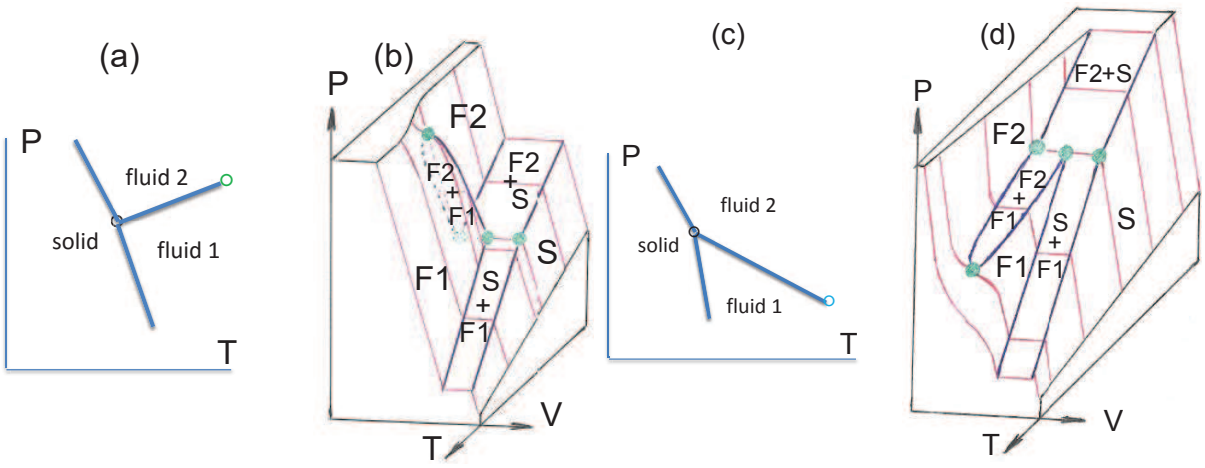

Figure 3. Schematic phase diagrams. (b)—thermodynamic $P(V,T)$ surface for the abnormal case when the slope of the melting curve $P(T)$ is negative and the slope of the fluid–fluid coexistence curve $P(T)$ is positive (a). (d)—thermodynamic $P(V,T)$ surface for the double abnormal case when the slopes of both melting and fluid–fluid coexistence curves $P(T)$ are negative (c). Isotherms are presented by red lines. S is solid, F is fluid.

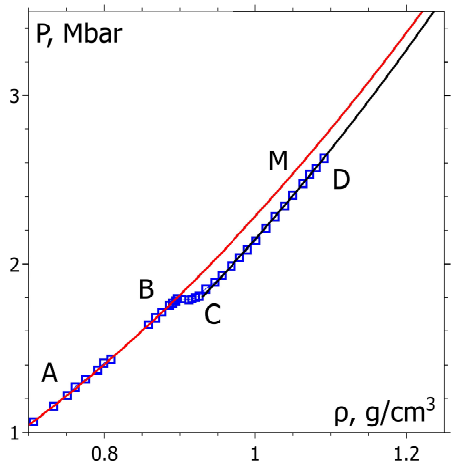

Figure 4. Warm dense hydrogen equation of state at $T = 1000$ K. A-B is fluid 1, C-D is fluid 2, B-C is two phase region [39]. B-M is an extrapolation, which describes the metastable state of fluid 1.

temperatures. Especially for experimental data [31], temperature estimations differ more than 2 times. Therefore, the observed discrepancy in temperature can be considered as indication to the weak contribution of the temperature-dependent part to the equation of state of hydrogen (deuterium) for the given values of pressure and density. Consequently, in this case, the isotherms of hydrogen are very close to the cold curve.

An explanation of discrepancy between data in figure 2 can be related to the possible metastability of the warm dense deuterium state observed in [32]. The existence of such states is demonstrated in figure 4. The metastability can be a result of the ultrafast process in Z machine.

6. Conclusions

An analysis is performed of fluid–fluid phase transitions at high temperatures with triple points on the melting curve. 3D thermodynamic $P(V,T)$ surfaces are constructed for normal and abnormal cases and related to experimental findings. The difference of the warm dense hydrogen with the "Brazhkin-type" case is emphasized. It is suggested that the state observed in [32] is a metastable one.

Acknowledgments

The authors would like to thank V Brazhkin, V Ryzhov and M Mochalov for useful discussions and comments. The work is supported by the Russian Science Foundation (grant No. 14-50-00124).

References

[1] Norman G E and Starostin A N 1970 *High Temp.* **8** 381–408
[2] Norman G É and Starostin A N 1970 *J. Appl. Spectrosc.* **13** 965–967
[3] Norman G E, Saitov I M and Stegailov V V 2015 *Contrib. Plasma Phys.* **55** 215–221
[4] Brazhkin V V, Voloshin R N and Popova S V 1989 *JETP Lett.* **50** 424–428
[5] Brazhkin V V, Popova S V and Voloshin R N 1997 *High Pressure Res.* **15** 267–305
[6] Brazhkin V V and Lyapin A G 2000 *Phys. Usp.* **43** 493–508
[7] Brazhkin V V, Funakoshi K, Kanzaki M and Katayama Y 2007 *Phys. Rev. Lett.* **99** 245901
[8] Brazhkin V V, Popova S V and Voloshin R N 1992 *Phys. Lett. A* **166** 383–387
[9] Katayama Y, Mizutani T, Utsumi W, Shimomura O, Yamakata M and Funakoshi K I 2000 *Nature* **403** 170–173
[10] Katayama Y, Inamura Y, Mizutani T, Yamakata M, Utsumi W and Shimomura O 2004 *Science* **306** 848–851
[11] Cadien A, Hu Q Y, Meng Y, Cheng Y Q, Chen M W, Shu J F, Mao H K and Sheng H W 2013 *Phys. Rev. Lett.* **110** 125503
[12] Chiba A, Funamori N, Nakayama K, Ohishi Y, Bennington S M, Rastogi S, Shukla A, Tsuji K and Takenaka M 2012 *Phys. Rev.* E **85** 021807
[13] Kirchhoff F, Kresse G and Gillan M J 1998 *Phys. Rev.* B **57** 10482–10495
[14] Korobenko V N and Rakhel A D 2012 *Phys. Rev.* B **85** 014208
[15] Brazhkin V V, Lyapin A G, Ryzhov V N, Trachenko K, Fomin Y D and Tsiok E N 2012 *Phys. Usp.* **55** 1061–1079
[16] Brazhkin V V, Fomin Y D, Lyapin A G, Ryzhov V N, Tsiok E N and Trachenko K 2013 *Phys. Rev. Lett.* **111** 145901 (*Preprint* 1305.3806)
[17] Ryltsev R E and Chtchelkatchev N M 2013 *Phys. Rev.* E **88** 052101
[18] Ryltsev R E and Chtchelkatchev N M 2014 *J. Chem. Phys.* **141** 124509
[19] Fomin Y D, Ryzhov V N, Tsiok E N, Brazhkin V V and Trachenko K 2014 *Sci. Rep.* **4** 7194
[20] Fomin Y D, Ryzhov V N, Tsiok E N and Brazhkin V V 2015 *Phys. Rev.* E **91** 022111
[21] Sokhan V P, Jones A, Cipcigan F S, Crain J and Martyna G J 2015 *Phys. Rev. Lett.* **115** 117801
[22] Weir S T, Mitchell A C and Nellis W J 1996 *Phys. Rev. Lett.* **76** 1860–1863
[23] Nellis W J, Weir S T and Mitchell A C 1999 *Phys. Rev.* B **59** 3434–3449
[24] Gregoryanz E, Goncharov A F, Matsuishi K, Mao H K and Hemley R J 2003 *Phys. Rev. Lett.* **90** 175701
[25] Loubeyre P, Celliers P M, Hicks D G, Henry E, Dewaele A, Pasley J, Eggert J, Koenig M, Occelli F, Lee K M, Jeanloz R, Neely D, Benuzzi-Mounaix A, Bradley D, Bastea M, Moon S and Collins G W 2004 *High Pressure Res.* **24** 25–31
[26] Deemyad S and Silvera I F 2008 *Phys. Rev. Lett.* **100** 155701
[27] Eremets M I and Troyan I A 2011 *Nat. Mater.* **10** 927–931
[28] Subramanian N, Goncharov A F, Struzhkin V V, Somayazulu M and Hemley R J 2011 *Proc. Natl. Acad. Sci. U. S. A.* **108** 6014–6019
[29] Dzyabura V, Zaghoo M and Silvera I F 2013 *Proceedings of the National Academy of Sciences* **110** 8040–8044
[30] Zaghoo M, Salamat A and Silvera I F 2015 *ArXiv e-prints* (*Preprint* 1504.00259)
[31] Fortov V E, Ilkaev R I, Arinin V A, Burtzev V V, Golubev V A, Iosilevskiy I L, Khrustalev V V, Mikhailov A L, Mochalov M A, Ternovoi V Y and Zhernokletov M V 2007 *Phys. Rev. Lett.* **99** 185001
[32] Knudson M D, Desjarlais M P, Becker A, Lemke R W, Cochrane K R, Savage M E, Bliss D E, Mattsson T R and Redmer R 2015 *Science* **348** 1455–1460
[33] Gryaznov V K, Iosilevskiy I L and Fortov V E 2004 *High-Pressure Shock Compression of Solids VII* (Springer-

Verlag New York) chap Thermodynamic Properties of Shock-Compressed Plasmas Based on a Chemical Picture, pp 437–489
[34] Tamblyn I and Bonev S A 2010 *Phys. Rev. Lett.* **104** 065702
[35] Kopyshev V P and Khrustalev V V 1980 *J. App. Mech. Tech. Phys.* **21** 113–118
[36] Ohta K, Ichimaru K, Einaga M, Kawaguchi S, Shimizu K, Matsuoka T, Hirao N and Ohishi Y 2015 *Sci. Rep.* **5** 16560
[37] McMahon J M, Morales M A, Pierleoni C and Ceperley D M 2012 *Rev. Mod. Phys.* **84** 1607–1653
[38] Morales M A, McMahon J M, Pierleoni C and Ceperley D M 2013 *Phys. Rev. Lett.* **110** 065702
[39] Lorenzen W, Holst B and Redmer R 2010 *Phys. Rev.* B **82** 195107